

## Modeling the $2\Omega$ Synchronous Signal for the TolTEC Imaging Polarimeter

ERIC VAN CAMP,<sup>1</sup> JASON AUSTERMANN,<sup>2</sup> SEAN BRYAN,<sup>3</sup> GILES NOVAK,<sup>1</sup>  
GIAMPAOLO PISANO,<sup>4</sup> AND GRANT WILSON<sup>5</sup>

<sup>1</sup>*Center for Interdisciplinary Exploration and Research in Astrophysics (CIERA) and Department of Physics and Astronomy, Northwestern University, Evanston, IL 60208, USA*

<sup>2</sup>*Quantum Sensors Group, National Institute of Standards and Technology, Boulder, CO, USA*

<sup>3</sup>*School of Electrical, Computer & Energy Engineering, Arizona State University, Tempe, AZ, USA*

<sup>4</sup>*School of Physics and Astronomy, Cardiff University, Cardiff, UK*

<sup>5</sup>*Department of Astronomy, University of Massachusetts, Amherst, MA 01003, USA*

### ABSTRACT

In this paper we present a method for modelling the  $2\Omega$  synchronous signal for TolTEC, a new polarimetric camera for the Large Millimeter Telescope. Along with other science goals, the polarimetric capability will be used to study the role of magnetic fields in star formation. TolTEC will observe in three bands centered at 300GHz, 220GHz, and 150GHz. Due to limitations of the novel KIDs detectors in use by TolTEC, power variations must be kept to below a 2K peak-to-peak variation in antenna temperature units while rapidly spinning the half-wave plate (HWP). The method presented in this paper evaluates current HWP designs by modelling the variation in antenna temperature at the detectors. For our current best HWP model, we find the antenna temperature variations are approximately 0.80K, 0.011K, and 2.0K for the high, medium, and low frequency bands respectively. Allowing for uncertainty in optical element parameters shows that the low frequency band falls outside of the 2K peak to peak power variation limit in approximately half of all cases studied. From these results, we conclude that the current HWP design must be altered if TolTEC is to operate in the lowest frequency band while the HWP is rapidly spinning. Our method may be useful for future study of other instruments.

### 1. INTRODUCTION

Although magnetic fields appear to permeate every galaxy, the origins and effects of the magnetic field are not well understood. What is known is that the magnetic field can interact with fully or partially ionized gas via Lorentz forces. Meanwhile, spinning, elongated interstellar dust grains tend to align with their long axis preferentially perpendicular to the ambient magnetic field, and so the field direction can be inferred from measurements of the polarization of the millimeter-wavelength thermal radiation from the grains ([Andersson et al. 2015](#); [Crutcher 2012](#)). The interaction

of magnetic fields with interstellar material may help to explain the low efficiency of star formation (McKee & Ostriker 2007).

Several telescopes and cameras already in operation use polarimetry, the measurement of polarized light, to map polarized emission from magnetically aligned dust grains and thereby answer questions regarding star formation. The *Planck* telescope, a space telescope operated by the European Space Agency (ESA), has measured the polarization of both interstellar clouds and cosmic microwave background radiation (Planck 2016). Due to the relatively coarse angular resolution of 5 arcminutes, the Planck results are useful for mapping large scale magnetic field features, but cannot map small scale magnetic field structures. The ALMA interferometer is capable of polarimetry measurements at sub-arcsecond resolution, down to the scale of individual protostellar sources (Hull et al. 2017). While ALMA polarimetry will be instrumental for understanding how magnetic fields influence star formation on small scales, and all-sky surveys such as Planck are helpful for understanding the role of large scale magnetic fields in star formation, the new TolTEC camera will be necessary to determine if there is any link between the large and small scale magnetic fields, and thereby gain a holistic view of star formation.

TolTEC will operate at the Large Millimeter Telescope (LMT) at the Sierra Negra observation site in Puebla, Mexico. The site is located at an altitude of 4,600m, allowing for excellent millimeter wavelength transmission year round. The LMT is collaborative effort between Mexico and the United States led by the Instituto Nacional de Astrofísica, Óptica y Electrónica (INAOE) and the University of Massachusetts at Amherst (UMass). With a 50m diameter dish, the LMT is the largest single dish telescope optimized to work in the millimeter wavebands. In the range of 1mm to 2mm, the telescope is diffraction limited to a resolution of 5-10 arcseconds allowing for detailed observations of nearby star forming regions.

The camera will be able to observe simultaneously in three bands centered at 1.1mm, 1.4mm, and 2.0mm (Bryan et al. 2018). Light is focused from the LMT primary and secondary mirrors through additional ambient temperature (warm) mirrors. From these additional mirrors, referred to as the warm optics, light passes through the half-wave plate (HWP), a device that rotates the polarization angle of incident linearly polarized light, and then into the cryostat. The cryostat contains the cold optics (comprised of dichroics to split incoming light into the three observing bands, lenses, and mirrors) and three arrays of detectors, one for each band. A more complete description of the optical design can be found in Bryan et al. (2018). The three bands have 1800, 900, and 450 pixels respectively, where each pixel has 2 detectors that detect orthogonal components of linearly polarized light. In total, there are over 6000 detectors in the TolTEC camera. Table 1 gives the wavelength, frequencies, and pixel count for the three bands.

In order to maximize the number of detectors, TolTEC uses kinetic inductance detectors (KIDs). A KID consists of a superconducting surface and resonator, and when

**Table 1.** TolTEC observing bands and pixel counts.

Band	Central Wavelength (mm)	Central Frequency (GHz)	Frequency Range (GHz)	Pixels
High Frequency	1.1	300	245-310	1800
Medium Frequency	1.4	220	195-245	900
Low Frequency	2.0	150	128-170	450

a photon is absorbed by the superconducting surface the frequency of the resonator is changed (Mauskopf 2018). By assigning each pixel in an array to a different initial resonant frequency, large arrays of detectors can be read in Fourier space by analyzing a single signal carried on a high-frequency cable running from the cryogenic detector array to room temperature. To minimize noise, KIDs must be operated at temperatures below 1K. One drawback of KIDs is that they are susceptible to  $1/f$  noise, where signals with low frequencies have the highest intensity of noise (as opposed to white noise, where all frequencies have the same amount of noise). This noise source can be mitigated by modulating the signal at a frequency above that which characterizes the bulk of the significant  $1/f$  noise. We accomplish this by rotating the HWP so that the polarization signal is modulated at  $4\Omega$ , that is, four times the speed of the spinning HWP.

By employing a continuously rotating half-wave plate (CRHWP), the effects of  $1/f$  noise are greatly reduced (Takakura et al. 2017). The HWP flips the angle of incoming polarized light across one of its two orthogonal axes. The result is that a rotation of the HWP by an angle  $\theta$  rotates the angle of polarization by  $2\theta$ . A rotation of 180 degrees returns the light to the same polarization state, so one full revolution of the HWP is equivalent to modulating the signal four times (a  $4\Omega$  modulation). The TolTEC HWP will be spun at 2 Hz, so the signal is modulated at a frequency of 8 Hz, reducing the effects of  $1/f$  noise introduced by the KIDs.

Besides the above mentioned  $4\Omega$  modulation, light reaching the detector varies in power at a frequency of  $2\Omega$ . This is because the orthogonal axes of the HWP have different emissivities and reflectivities. If the power level fluctuates too much the KIDs readout electronics will lose lock on the individual resonators' frequencies. The  $4\Omega$  power variations are small compared to the HWP  $2\Omega$  signal. To avoid losing lock, the total peak to peak power variation from the  $2\Omega$  HWP rotation cannot exceed 2K in antenna temperature. This varying power due to spinning the HWP is known as the  $2\Omega$  *synchronous signal*. The present paper introduces a method for modelling the  $2\Omega$  synchronous signal for the TolTEC camera. (Our python code is given in appendix B.) Based on the results of this synchronous signal calculation we can evaluate designs for the HWP prior to its manufacture.

## 2. MODELING THE SYNCHRONOUS SIGNAL

In this work, power is described using antenna temperature as it is defined in [Draine \(2011\)](#):

$$T_A(\nu) \equiv \frac{c^2}{2k\nu^2} I_\nu \quad (1)$$

Antenna temperature is useful because it is linear with intensity, and also gives an approximation of the temperature the object would have were it emitting like a black-body in the small  $\nu$  limit. Power can then be calculated from the antenna temperature, via

$$P = I_\nu \Delta\nu A \Omega = \frac{2k\nu^2}{c^2} T_A \Delta\nu A \Omega \quad (2)$$

where  $A$  is the telescope collecting area,  $\Omega$  is the beam solid angle for a given band, and  $\Delta\nu$  is the frequency range of the band. In the Rayleigh-Jeans limit of small  $\nu$ , power is given by

$$P = \frac{2k\nu^2}{c^2} \epsilon T_{\text{physical}} \Delta\nu A \Omega \quad (3)$$

where  $\epsilon$  is the emissivity of the object. It is clear from equations (2) and (3) that for our optical elements in the Rayleigh-Jeans limit we can use

$$T_A = \epsilon T_{\text{physical}} \quad (4)$$

The one exception to this approximation is for the detectors in the cryostat at  $0.1K$  as this is outside of the domain of the validity of the Rayleigh-Jeans approximation. However, the power from the  $0.1K$  detectors is negligible, and so we can choose to disregard this discrepancy.

We use the *am* atmospheric model to calculate the antenna temperature of the sky when observing at the LMT site ([Paine 2018](#)). We initially assume water vapor is at the 25<sup>th</sup> percentile level, though we later explore other percentile levels. The antenna temperature as estimated for each frequency between 100 GHz and 320 GHz by the *am* model is shown in figure 1.

To model the power reaching the TolTEC detectors we need to assume values for the physical temperatures, emissivities, and reflectivities of each optical element. The temperatures and emissivities of the LMT primary mirrors, secondary mirrors, and warm optics are taken from [Bryan et al. \(2018\)](#). Following this reference, the primary and secondary mirrors are at 273 K with a combined effective emissivity of 6%. The warm optics (ambient temperature polished mirrors) are at 290 K with a total emissivity of 3%. The half-wave plate is modelled using frequency-dependent emissivity and reflectivity values obtained from models developed at Cardiff University. For our current best HWP design, the frequency dependent transmission, absorption, and reflection for the two axes of the HWP are given in figure 2. For other optical elements, we make initial assumptions based on best guesses for the finished camera. We assume the pressure window of the cryostat is a perfect transmitter, with an emissivity

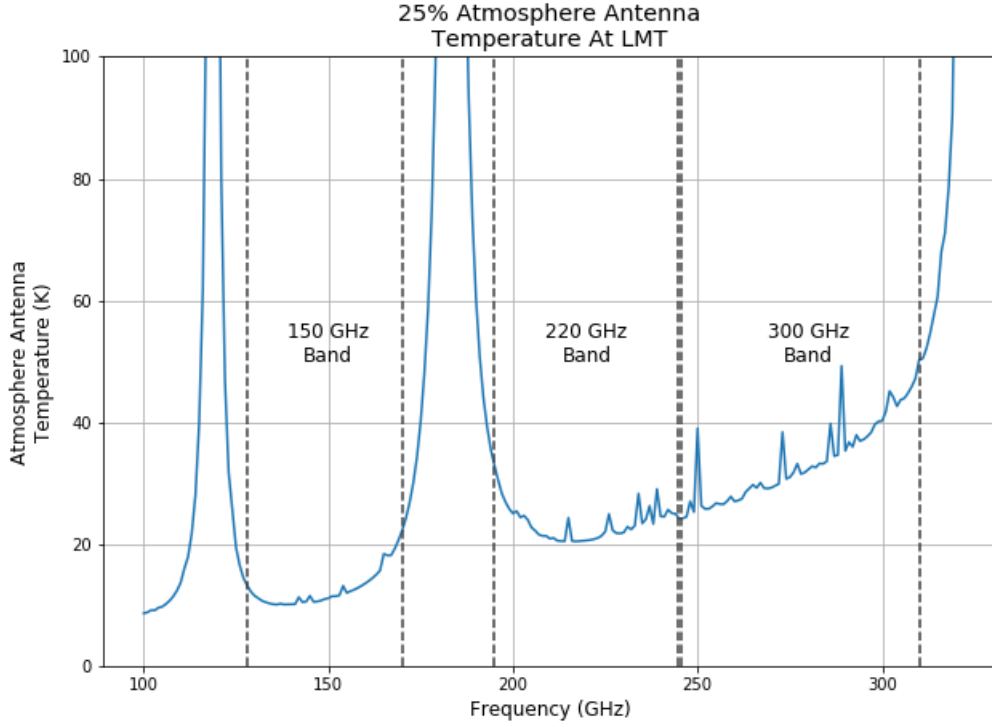


**Figure 1.** The antenna temperature assuming 25th percentile water vapor as predicted by the *am* atmospheric model (Paine 2018). The three observing bands for the TolTEC camera are labelled with vertical dashed lines.

**Table 2.** List of initial assumptions made in synchronous signal calculation.

Optical Element	Physical Temperature	Emissivity	Reflectivity	Reflection Temperature
Atmosphere <sup>a</sup>	-	-	-	-
Telescope mirrors	273K <sup>b</sup>	6% <sup>b</sup>	-	-
Warm Optics	290K <sup>b</sup>	3% <sup>b</sup>	-	-
HWP	290K	see fig. 2	see fig. 2	45K
Pressure Window	290K	0%	0%	45K
Cold Optics	5.5K	65%	-	-
Detector	0.1K	20%	-	-

<sup>a</sup>Antenna temperatures taken directly from *am* atmospheric model shown in fig. 1

<sup>b</sup>Values taken from Bryan et al. (2018)

0%. For the cold optics, we assume an average temperature of 5.5K and an emissivity of 65%. We assume the detectors are at 0.1 K and have an emissivity of 20%. A list of the above assumptions and others made in this calculation is given in table 2.

The synchronous signal calculation method presented in this paper computes the antenna temperature of radiation as it passes through each optical element (or group

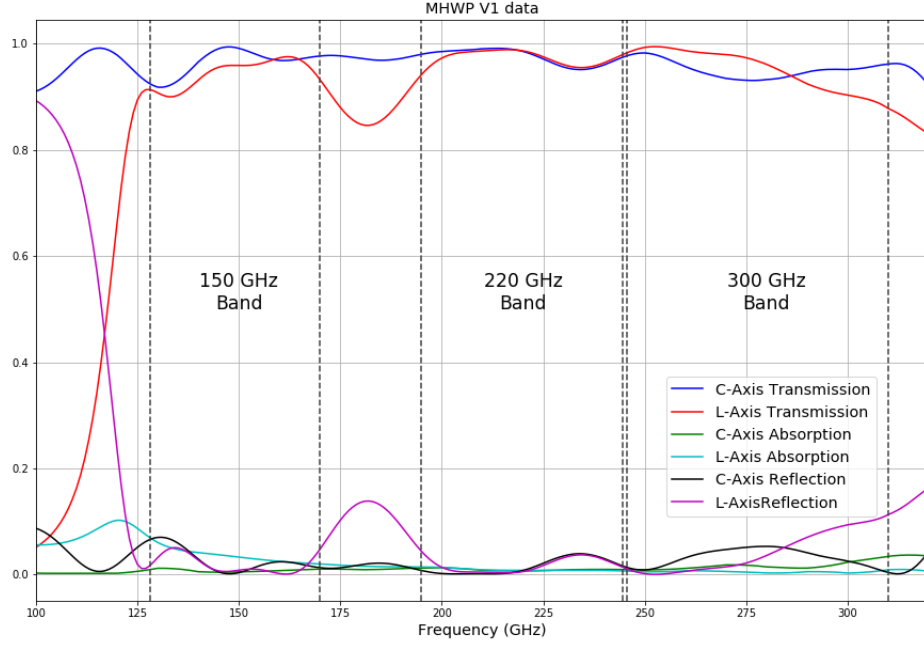


**Figure 2.** Transmission, absorption, and reflection for two orthogonal HWP axes, from Cardiff University HWP model. Vertical dashed lines indicate the boundaries of the low, medium, and high frequency bands.

of optical elements) of the LMT and TolTEC. Emission and reflection of the primary and secondary mirrors, warm optics, HWP, pressure window, cold optics, and detectors are all considered. Starting from the sky antenna temperature shown in figure 1, we calculate antenna temperature of the sky plus mirror emission, then antenna temperature of sky, mirror, and warm optics emission, etc., sequentially calculating antenna temperatures until the antenna temperature at the detector is known. This process is illustrated in figure 3, and the complete code is given in the appendix and can be found online<sup>1</sup>. Note that mirrors are modelled as lenses with reflectivity of zero. The calculation of the temperature seen at the detector is done twice, once for the C-axis and again for the L-axis of the HWP. The L-axis temperature subtracted from the C-axis temperature, the average temperature, and the fractional difference, are output as a function of frequency. Note that thermal radiation originating inside the cryostat but traveling outward through the pressure window can find its way back to the detectors via a reflection from the HWP. The fourth row of the rightmost column of table 2 gives our best estimate for the antenna temperature of this outgoing radiation as it exits the cryostat. The caption to figure 3 explains in details how this effect is modelled.

<sup>1</sup> <https://github.com/ervc/TolTEC-HWP>

**Table 3.** Band averaged antenna temperature difference (C-L) for each band.

Band	Frequency Range (GHz)	$\Delta T_{\text{band}}(K)$	$T_{\text{band, avg}}$	Fractional difference	Average loading (pW)
Low	128-170	-1.99	14.6	13.7%	13.1
Medium	195-245	0.0110	16.4	0.0611%	16.6
High	245-310	0.803	18.9	4.03%	25.7

### 3. RESULTS

Graphs of the temperature difference, average temperature, and fractional temperature difference are shown in figure 4. Band averaged results are obtained by taking an unweighted average of each quantity within each passband, and these are shown in table 3. Finally, the loading on the detector for each of the three bands is calculated using equation 2, where  $T_A$  is the average antenna temperature at the detectors. To calculate the loading, the central frequency of the band was used for  $\nu$ , and  $\Delta\nu$  is the width of the band.  $A$  is the area of the LMT primary dish ( $A = \pi(25m)^2$ ) and the observing solid angle can be calculated from the FWHM given by [Bryan et al. \(2018\)](#). The loading values are given in table 3.

As discussed in the following section, we also explored the effects of varying parameters such as emissivity, reflection temperature, and antenna temperatures of the atmosphere, HWP, cold optics, and detectors. The values we explored are listed in table 4. The antenna temperature difference curves that result from varying each of these values individually are graphed in appendix A, and tables giving the corresponding band averaged differences are also given there. While these single-parameter variations give insight into the model, we must also consider the effects of varying multiple parameters. Accordingly, we varied five parameters, using three different values for each, resulting in  $3^5 = 243$  possible combinations for each frequency band. A histogram showing the temperature difference results from all 243 possible variations is given in figure 5. This result is discussed in next section.

### 4. CONCLUSION

The results shown in figure 4 and table 3 employ the initial assumptions listed in table 2. Using these assumptions, the current HWP design is marginal with respect to the 2K peak to peak requirement on power variation. Specifically, the low frequency band barely satisfies the requirement. However, there are likely variations in these assumptions that will change the  $\Delta T_{\text{band}}$  for all three bands. For example, we expect the atmospheric percentile to change on a day to day basis, which will change the resulting peak to peak power variation. Additionally, because the instrument is still being fabricated, parameters not related to the LMT telescope itself remain unknown (see rows 2-5 of table 4).



**Table 4.** Variations of assumptions made in synchronous signal calculation.

Optical Element	Parameter changed	Values used
Atmosphere	Water vapor percentile	5, <b>25</b> , 50
HWP	Reflection Temperature	25K, <b>45K</b> , 65K
Cold Optics	Emissivity	45%, <b>65%</b> , 85%
”	Physical Temperature	4K, <b>5.5K</b> , 10K
Detector	Emissivity	10%, <b>20%</b> , 30%

Parameter values explored to produce figure 5. By considering three different values for each of 5 parameters, 243 combinations were tested. Any parameters not listed were not changed from the initial assumptions given in table 2. In rightmost column, initial assumptions are indicated with bolding.

Allowing for variations in unknown parameters identified in table 4, figure 5 shows that roughly half of these variations result in the low band having a peak to peak power variation of greater than 2K. In all of the cases where the low frequency band fails, the  $\Delta T_{\text{band}}$  value is negative, meaning the L-axis antenna temperature is higher than the C-axis temperature. This is due to the fact that that in the low band the L-axis absorption is higher than the C-axis absorption (see figure 2). This results in the 290K emission making up a larger percentage of the read-out antenna temperature, raising the antenna temperature. In the high frequency band, the opposite is true: the C-axis absorption is higher than the L-axis absorption, resulting in larger positive  $\Delta T_{\text{band}}$  values. In the high frequency band, however, the peak to peak antenna temperature variation is never greater than 2K. The failure of the low frequency band to meet the 2 K peak-to-peak requirement for roughly half of the parameter combinations shows that successful polarimetry in this band with the HWP design shown here is doubtful.

In general, the HWP is manufactured to maximize transmission and minimize emission and reflection. However, the problem with our low frequency band arises from differences in absorption and transmission, and specifically is related to the relatively larger L-axis absorption. Thus, it may be possible to mitigate the problem either by lowering the L-axis absorption or by raising the the C-axis absorption. This would reduce the difference in antenna temperature at the detectors while sacrificing some signal and increasing the amount of background. Unfortunately, however, it may difficult or impossible to affect absorption and in only one of the three observing bands. Design changes aimed at reducing the difference in absorption in one band may also affect the results for the other two bands.

Alternatively, TolTEC could operate in a mode where polarimetry data are collected for only the two highest frequency bands. Most of our science targets emit most strongly in these two bands. Even while sacrificing one observing band, TolTEC



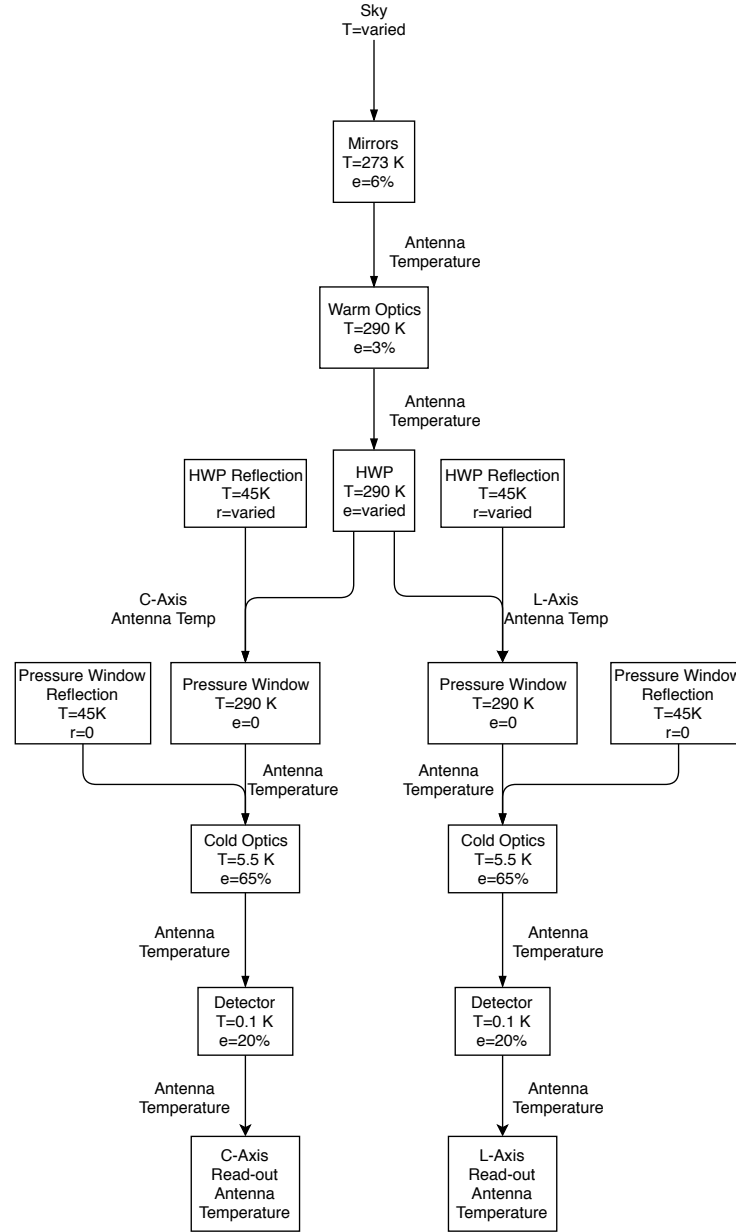
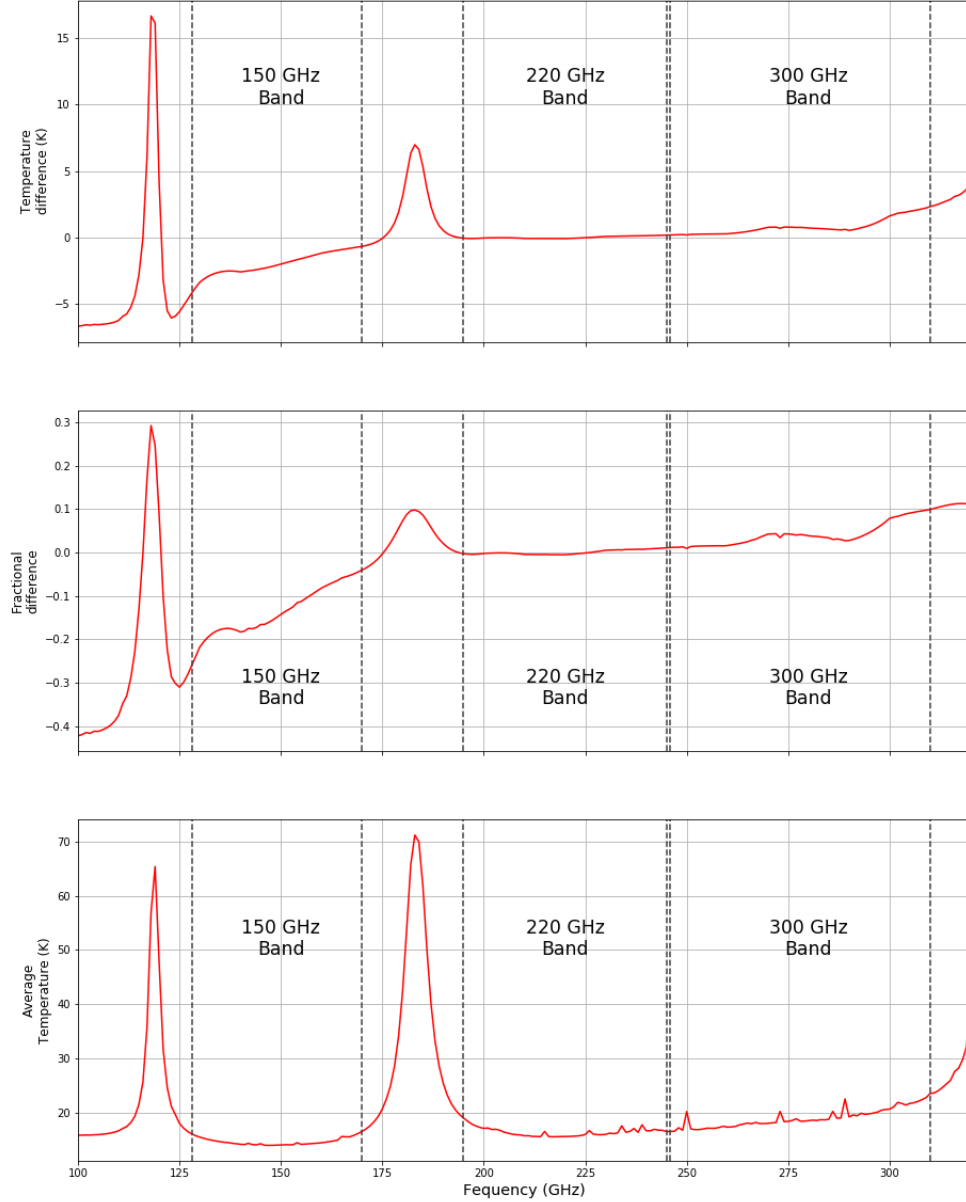


**Figure 3.** Flow chart illustrating operation of the synchronous signal calculation described in this paper. The antenna temperature at each step is calculated by multiplying the transmission times the antenna temperature from the previous step, adding the emissivity times the element temperature, and (for the HWP and pressure window only) further adding the reflectivity times the "reflection temperature". E.g. the antenna temperature of radiation after passing through the mirrors is  $(\text{Sky Temp})(0.94) + (273 \text{ K})(0.06)$ . This calculation is done twice, once for the C-axis and once for the L-axis and the resulting antenna temperatures are then differenced.



$2\Omega$  synchronous signals for TolTEC  
as calculated by our code

**Figure 4.** The polarization dependent difference in antenna temperature at the detectors due to differential reflection and absorption of the HWP. Results shown here employ the initial assumptions given in table 2. This polarization dependent difference is also referred to as the  $2\Omega$  synchronous signal. *Top*: detector antenna temperature difference in Kelvin. *Middle*: fractional difference in antenna temperature based on average temperature. *Bottom*: average antenna temperature for both HWP axes. Observing bands are indicated with vertical dashed lines.

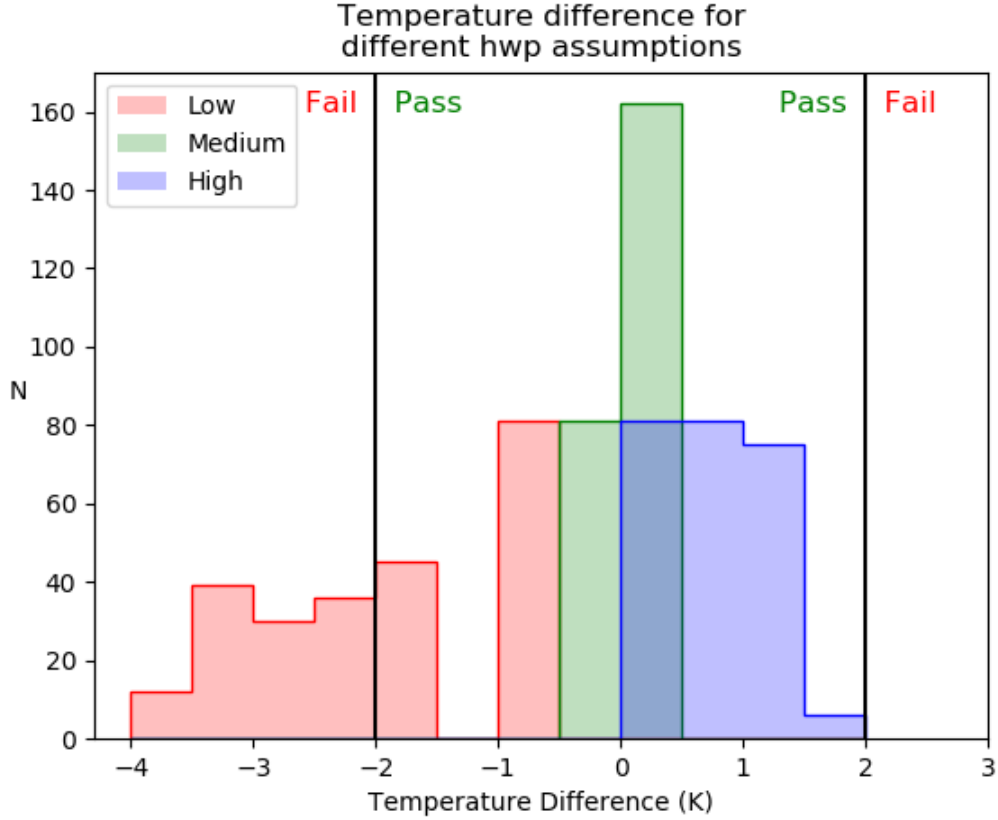


**Figure 5.** Histogram showing the  $\Delta T_{\text{band}}$  for each possible combination of variations listed in table 4.  $\Delta T_{\text{band}}$  is calculated by subtracting the L-axis antenna temperature from the C-axis antenna temperature. Vertical lines showing a peak to peak variation in antenna temperature of 2K are shown. Results for the low frequency band are shown in red, medium frequency band in green, and high frequency band in blue. The number of trials in each bin is given on the y-axis and temperature difference at the detectors in Kelvin is given on the x-axis. Bin width is 0.5K.

would remain a powerful tool for polarimetry of interstellar material and star forming regions. However, there is interest in studying how polarization of light is dependent on wavelength, as this could give further insight into star formation (Gandilo et al. 2016).

The model described in this paper provides an effective tool for calculating differential power reaching detectors for cameras using a CRHWP. Currently, the model is optimized for TolTEC, but its modules and inputs can easily be changed to adapt it to other applications.

## 5. ACKNOWLEDGEMENTS

This work was supported by the Northwestern Weinberg College of Arts and Sciences Research Grant and from the NASA Illinois Space Grant. TolTEC is supported by a grant to the University of Massachusetts from the National Science Foundation.

## REFERENCES

- Andersson, B.-G., Lazarian, A., & Vaillancourt, J.E. 2015, ARA&A, 53, 501-39
- Bryan, S., Austermann, J., Ferrusca, D., et al. 2018, SPIE Astronomical Telescopes and instrumentation, 10708, doi:10.1117/12.2314130
- Crutcher, R.M. 2012, ARA&A, 50, 29-63
- Draine, B.T. 2011, Physics of the Interstellar and Intergalactic Medium, (Princeton, NJ: Princeton University Press)
- Gandilo, N.N., Ade, P.A.R., Angilè, F.E., et al. 2016, ApJ, 824, 24
- Hull, C.L.H., Girart, J.M., Tychoniec, L., et al. 2017, ApJ, 847, 92
- Mauskopf, P.D. 2018, PASP, 130, 990
- McKee, C.F. & Ostriker, E.C. 2007, ARA&A, 45, 565-687
- Paine, S. 2018, The *am* atmospheric model, v10.0, Zenodo, doi:10.5281/zenodo.1193771
- Planck Collaboration 2016, A&A, 594, A13
- Takakura, S., Aguilar, M., Akiba, Y., et al. 2017, JCAP, 05, 008
- Zweibel, E.G. & Heiles, C. 1997, Nature, 385, 131-136

## APPENDIX

## A. RESULTS OF VARYING ONE ASSUMPTION AT A TIME

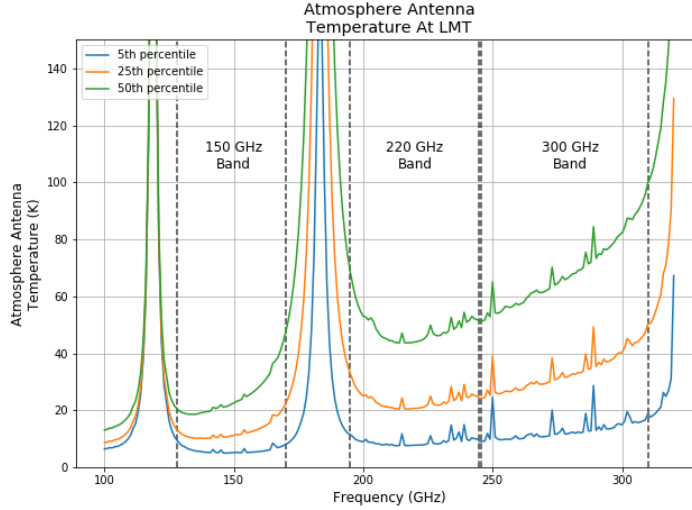


**Figure 6.** Antenna temperatures for 5th, 25th, and 50th percentile atmospheres for model shown in figure 1.

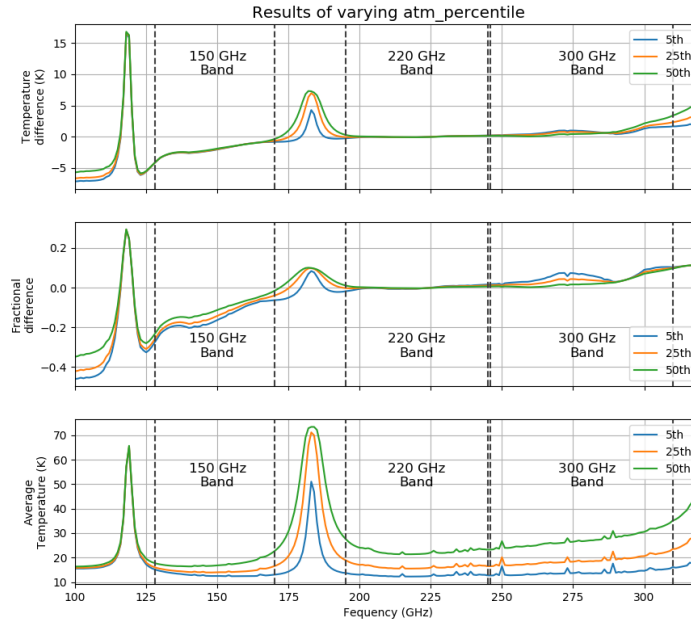


**Figure 7.** Results of varying only atmosphere percentiles as given in figure 6. Graphs show temperature difference, fractional difference, and average temperature as in figure 4.

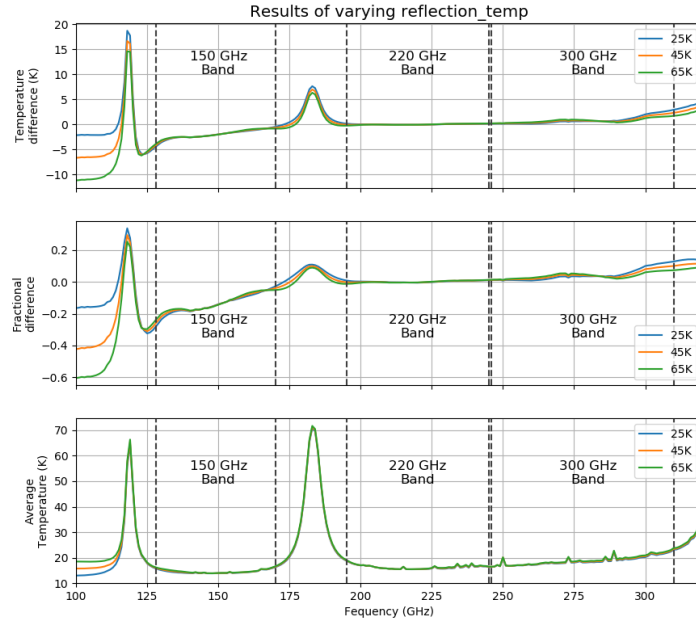


**Figure 8.** Results of varying only HWP reflection temperature. Graphs show temperature difference, average temperature and fractional difference as in figure 4.

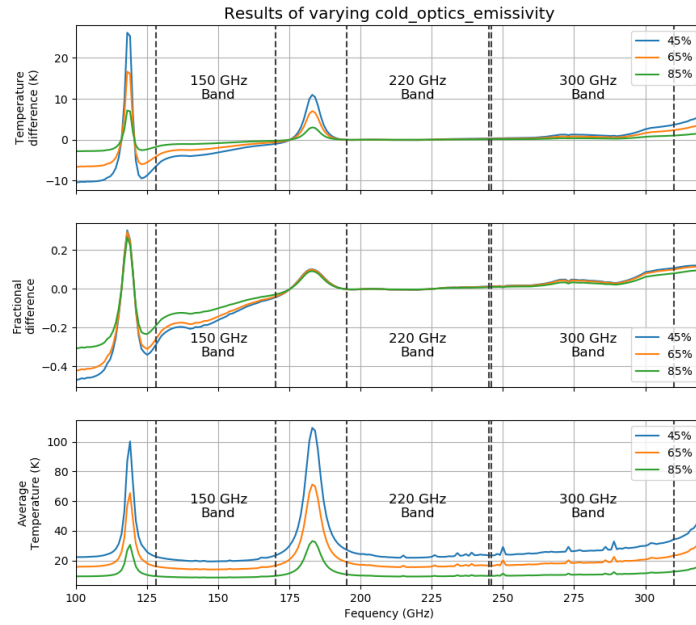


**Figure 9.** Results of varying only cold optics emissivity. Graphs show temperature difference, average temperature and fractional difference as in figure 4.

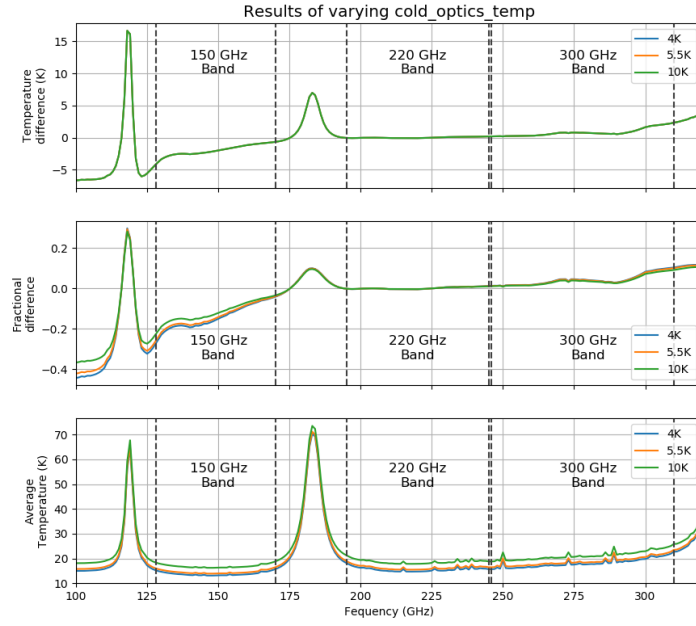


**Figure 10.** Results of varying only cold optics temperature. Graphs show temperature difference, average temperature and fractional difference as in figure 4.

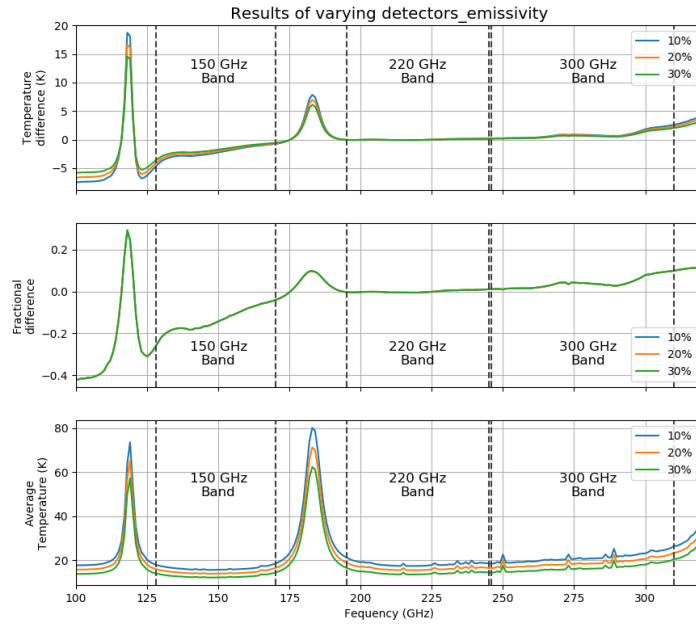


**Figure 11.** Results of varying only detector emissivity. Graphs show temperature difference, average temperature and fractional difference as in figure 4.



**Table 5.** Band average results for variations in assumption.

Band	$\Delta T_{\text{band}}(K)$	$T_{\text{band, avg}}$	Fractional difference	Average loading (pW)
Initial Assumptions				
Low	-1.989	14.62	-0.1366	13.06
Medium	0.01096	16.38	0.0006114	16.59
High	0.8029	18.94	0.04032	25.65
Atmosphere percentile: 5th				
Low	-2.022	12.97	-0.1538	11.68
Medium	-0.0007532	12.80	-0.0001178	13.11
High	0.7704	13.95	0.05419	18.93
Atmosphere percentile: 50th				
Low	-1.928	17.68	-0.1126	15.65
Medium	0.03046	22.73	0.001174	22.86
High	0.8474	27.46	0.02800	37.25
HWP reflection temp: 25K				
Low	-2.033	14.49	-0.1410	13.03
Medium	0.02407	16.29	0.001344	16.55
High	0.8615	18.73	0.04309	25.33
HWP reflection temp: 65K				
Low	-1.945	14.75	-0.1323	13.08
Medium	-0.002156	16.47	-0.0001188	16.62
High	0.7444	19.15	0.03768	25.97
cold optics emissivity: 45%				
Low	-3.126	20.45	-0.1536	18.15
Medium	0.01722	23.21	0.00067047	23.37
High	1.262	27.24	0.04389	36.78

*Table 5 continued on next page*

**Table 5** (*continued*)

Band	$\Delta T_{\text{band}}(K)$	$T_{\text{band, avg}}$	Fractional difference	Average loading (pW)
cold optics emissivity: 85%				
Low	-0.8525	8.792	-0.09720	7.958
Medium	0.004696	9.545	0.0004614	9.805
High	0.3441	10.64	0.03106	14.52
cold optics temp: 4K				
Low	-1.989	13.84	-0.1443	12.33
Medium	0.01096	15.60	0.0006388	15.75
High	0.8029	18.16	0.04197	24.56
cold optics temp: 10K				
Low	-1.989	16.96	-0.1176	15.25
Medium	0.01096	18.72	0.0005417	19.08
High	0.8029	21.28	0.03605	28.92
Detectors emissivity: 10%				
Low	-2.24	16.44	-0.1367	14.68
Medium	0.01233	18.41	0.0006118	18.65
High	0.9033	21.30	0.04034	28.84
Detectors emissivity: 30%				
Low	-1.741	12.81	-0.1365	11.44
Medium	0.009589	14.34	0.0006110	14.53
High	0.7026	16.59	0.04029	22.46

## B. SYNCHRONOUS SIGNAL CODE

```

#rflag and aflag tell the function whether to include reflectivities
#and absorptivities
#if rflag == 0, then all reflectivity values are considered to be zero,
#same for aflag
#if rflag == 1, then reflectivities are taken from optical element csv,
#same for aflag
#aflag has the option of aflag == -1, this sets only the hwp absorptivity
#to zero
def before_hwp(Tin, file, rflag, aflag):
    #make a new empty list for output temperatures
    Tout=[]

    #note this file assumes columns are in order
    #Frequency, Absorption, Reflection, T-reflected, T-absorbed
    with open(file) as csv_file:
        csv_reader = csv.reader(csv_file, delimiter=',')
        line_count = 0
        for row in csv_reader:
            #skip header row
            if line_count == 0:
                line_count += 1
            else:
                #again, assuming correct order of columns.
                Indices can be changed, but all files
                #should be consistent with ordering of columns
                a=float(row[1])
                r=float(row[2])
                if rflag == 0:
                    r = 0
                if aflag == 0:
                    a = 0
                t=1-a-r
                T_a = float(row[4])
                T_r = float(row[3])

                Temp = t*Tin[line_count-1]+a*T_a+r*T_r
                Tout.append(Temp)

                line_count+=1

```

```
return(Tout)
```

```
def during_hwp(Tin, file, rflag, aflag):
```

```
Tout_perp=[]
```

```
Tout_para=[]
```

```
'''Right now this has been designed with the same file for which I
digitized HWP absorptions so the first column is Frequency, then 8
columns of data, then columns 9 and 10 are average absorptions
for the two axes (arbitrarily assigned parallel or perpendicular).
Column 11 is the temperature the HWP emits at.
```

```
There is currently
```

```
no reflection data so reflectivity is not included at all in the
code, though it shouldn't be hard to add should that data be available
with open(file) as csv_file:
```

```
    csv_reader = csv.reader(csv_file, delimiter=',')
```

```
    line_count = 0
```

```
    for row in csv_reader:
```

```
        #skip to freq=100
```

```
        if line_count < 92:
```

```
            line_count += 1
```

```
        else:
```

```
            a_perp=float(row[3])
```

```
            a_para=float(row[6])
```

```
            r_perp=float(row[2])
```

```
            r_para=float(row[5])
```

```
            if rflag == 0:
```

```
                r_perp = 0
```

```
                r_para = 0
```

```
            if aflag == 0 or aflag == -1:
```

```
                a_perp = 0
```

```
                a_para = 0
```

```
            t_perp=1-a_perp-r_perp
```

```
            t_para=1-a_para-r_para
```

```
            T_emit = float(row[14])
```

```
            T_r = float(row[15])
```

```
Temp_perp =
```

```

        t_perp*Tin[line_count-92]+a_perp*T_emit+r_perp*T_r
Temp_para =
        t_para*Tin[line_count-92]+a_para*T_emit+r_para*T_r

    Tout_perp.append(Temp_perp)
    Tout_para.append(Temp_para)

    line_count+=1
return(Tout_perp, Tout_para)

#this is the same as the before_hwp function but is made to take in two
Temperatures and output two Temperatures
def after_hwp(Tin_perp, Tin_para, file, rflag, aflag):
    Tout_perp=[]
    Tout_para=[]

    with open(file) as csv_file:
        csv_reader = csv.reader(csv_file, delimiter=',')
        line_count = 0
        for row in csv_reader:
            if line_count == 0:
                line_count += 1
            else:
                a=float(row[1])
                r=float(row[2])
                if rflag == 0:
                    r = 0
                if aflag == 0:
                    a = 0
                t=1-a-r

                T_a = float(row[4])
                T_r = float(row[3])

                Temp_perp = t*Tin_perp[line_count-1] + a*T_a + r*T_r
                Temp_para = t*Tin_para[line_count-1] + a*T_a + r*T_r

                Tout_perp.append(Temp_perp)
                Tout_para.append(Temp_para)

                line_count+=1

```

```

    return(Tout_perp , Tout_para)

def picowatt_calc(lower_nu , upper_nu , freq , T_A, FWHM):
    k = 1.38e-23
    c = 3e8
    A = pi*(25**2)

    nu = (upper_nu+lower_nu)/2
    d_nu = upper_nu-lower_nu

    if int(nu) != nu:
        nu += 0.5
    index = freq.index(nu)
    Temp = T_A[index]

    nu = nu*10**9
    d_nu = d_nu*10**9

    FWHM_rad = (FWHM/3600)*(pi/180)
    HWHM = FWHM_rad/2
    Omega = pi*HWHM**2

    I_num = 2*k*nu**2
    I_den = c**2

    W = (I_num/I_den)*Temp*d_nu*A*Omega
    pW = W*10**12

    return(pW)

def hwp_analysis( file_list , rflag , aflag ):

    #loop through each file
    for file in file_list:
        #this if statement checks if the output is a list ,
        #All the files before the HWP should output a list of
        #temperatures , after the HWP the output will be a
        #tuple including a temperature for the parallel
        #axis and a temperature for the perpendicular axis
        if 'LMT' in file:
            f = open(file , 'r')

```

```

data = f.readlines()
T_eff=[]
for line in data:
    elements=line.split()
    T_eff.append(float(elements[3]))
elif type(T_eff) == list:
    #if file is not the hwp file, this title can be changed
    #if need be
    if file[:5] != 'model':
        T_eff = before_hwp(T_eff, file, rflag, aflag)
        #T_eff_list.append(T_eff[10])
    else:
        T_eff = during_hwp(T_eff, file, rflag, aflag)
        T_perp = T_eff[0]
        T_para = T_eff[1]
        #T_eff_list.append([T_perp[10], T_para[10]])
#after the HWP T_eff is a tuple, so the code used needs to
#calculate twice.
    else:
        T_perp, T_para = after_hwp(T_perp, T_para, file, rflag, aflag)
        #T_eff_list.append([T_perp[10], T_para[10]])

#create empty lists for the analysis of Temperature data once
#all the files are looped through
T_diff = []
T_avg = []
differential = []
for i in range(len(T_perp)):
    #calculates difference and average T at each frequency
    T_diff.append(T_perp[i] - T_para[i])
    T_avg.append((T_perp[i]+T_para[i])/2)

for i in range(len(T_diff)):
    #finally, calculates the fractional differential (difference/average)
    differential.append(T_diff[i]/T_avg[i])

#make a list of frequencies
frequency = [i for i in range(100,321,1)]

#get band averages

```



```

differential_low_list = [differential[i] for i in
range(len(frequency)) if frequency[i] >= 128 and frequency[i] <= 170]
differential_med_list = [differential[i] for i in
range(len(frequency)) if frequency[i] >= 195 and frequency[i] <= 245]
differential_high_list = [differential[i] for i in
range(len(frequency)) if frequency[i] >= 245 and frequency[i] <= 310]

diff_low_band = np.mean(differential_low_list)
diff_med_band = np.mean(differential_med_list)
diff_high_band = np.mean(differential_high_list)

T_diff_low_list = [T_diff[i] for i in range(len(frequency)) if
frequency[i] >= 128 and frequency[i] <= 170]
T_diff_med_list = [T_diff[i] for i in range(len(frequency)) if
frequency[i] >= 195 and frequency[i] <= 245]
T_diff_high_list = [T_diff[i] for i in range(len(frequency)) if
frequency[i] >= 245 and frequency[i] <= 310]

T_diff_low_band = np.mean(T_diff_low_list)
T_diff_med_band = np.mean(T_diff_med_list)
T_diff_high_band = np.mean(T_diff_high_list)

T_avg_low_list = [T_avg[i] for i in range(len(frequency)) if
frequency[i] >= 128 and frequency[i] <= 170]
T_avg_med_list = [T_avg[i] for i in range(len(frequency)) if
frequency[i] >= 195 and frequency[i] <= 245]
T_avg_high_list = [T_avg[i] for i in range(len(frequency)) if
frequency[i] >= 245 and frequency[i] <= 310]

T_avg_low_band = np.mean(T_avg_low_list)
T_avg_med_band = np.mean(T_avg_med_list)
T_avg_high_band = np.mean(T_avg_high_list)

picowatt_low = picowatt_calc(128,170,frequency,T_avg,9.5)
picowatt_med = picowatt_calc(195,245,frequency,T_avg,6.3)
picowatt_high = picowatt_calc(245,310,frequency,T_avg,5)

#write outputs to csv file
with open('output.csv', 'w', newline='') as csvfile:
    write_file = csv.writer(csvfile, delimiter=',')
    row=0

```

```

for i in range(len( differential)+1):
    if row==0:
        write_file.writerow([ 'Frequency_(GHZ) ', 'T_diff_(K) ',
                                'T_avg_(K) ', 'fractional_difference '])
        row+=1
    else:
        write_file.writerow([ frequency[i-1],
                                T_diff[i-1],T_avg[i-1],differential[i-1]])
        row+=1

with open('band_avg_out.csv', 'w', newline='') as csvfile:
    write_file = csv.writer(csvfile, delimiter=',')
    write_file.writerow([ 'Band', 'Frequency_(GHZ) ',
                            'Delta_T_band_(K) ', 'T_band_avg_(K) ',
                            'fractional_difference_(band_avg) ', 'Picowatt_loading '])
    write_file.writerow([ 'Low', '128-170 ', T_diff_low_band,
                            T_avg_low_band, diff_low_band, picowatt_low])
    write_file.writerow([ 'Medium', '195-245 ', T_diff_med_band,
                            T_avg_med_band, diff_med_band, picowatt_med])
    write_file.writerow([ 'High', '245-310 ', T_diff_high_band,
                            T_avg_high_band, diff_high_band, picowatt_high])

delta_t_band_list=[T_diff_low_band, T_diff_med_band, T_diff_high_band]
t_band_avg_list = [T_avg_low_band, T_avg_med_band, T_avg_high_band]
band_fractional_list=[diff_low_band, diff_med_band, diff_high_band]
picowatt_list = [picowatt_low, picowatt_med, picowatt_high]

#Returned values returned are in decimal form.
return([frequency, T_diff, T_avg, differential,
        delta_t_band_list, t_band_avg_list,
        band_fractional_list, picowatt_list])

```